Growth form defines physiological photoprotective capacity in intertidal benthic diatoms

Alexandre Barnett, Vona Méléder, Lander Blommaert, Bernard Lepetit, Wim Vyverman, Koen Sabbe, Christine Dupuy, Johann Lavaud

To cite this version:

Alexandre Barnett, Vona Méléder, Lander Blommaert, Bernard Lepetit, Wim Vyverman, et al.. Growth form defines physiological photoprotective capacity in intertidal benthic diatoms. ISME Journal, Nature Publishing Group, 2015, 9, pp.32-45. <10.1038/ismej.2014.105>. <hal-01110925>

HAL Id: hal-01110925
https://hal.archives-ouvertes.fr/hal-01110925

Submitted on 29 Jan 2015

Growth form defines physiological photoprotective capacity in intertidal benthic diatoms

Alexandre Barnett[1], Vona Méléder[1,2], Lander Blommaert[1,3], Bernard Lepetit[1#], Pierre Gaudin[1,2$], Wim Vyverman[3], Koen Sabbe[3], Christine Dupuy[1] & Johann Lavaud[1*]

[1] UMR7266 LIENSs 'Littoral, Environnement et Sociétés', CNRS/Université de La Rochelle, Institut du Littoral et de l'Environnement, 2 rue Olympe de Gouges, 17000 La Rochelle, France.

[2] UPRES EA 2160 MMS 'Mer, Molécules, Santé', Université de Nantes, Faculté des Sciences et Techniques, 2 rue de la Houssinière, BP 92208, 44322 Nantes cedex 3, France.

[3] Laboratory of Protistology & Aquatic Ecology, Department of Biology, Ghent University, Krijgslaan 281-S8, B-9000 Ghent, Belgium.

[*] Corresponding author:

UMR 7266 'LIENSs', CNRS/Université de La Rochelle, Institut du Littoral et de l'Environnement (ILE), 2 rue Olympe de Gouges, 17000 La Rochelle, France

Phone: +33-(0)5-46-50-76-45, Fax: +33-(0)5-46-45-82-64, E-mail: johann.lavaud@univ-lr.fr

[#] Current address: Group of Plant Ecophysiology, Department of Biology, University of Konstanz, Universitätsstraße 10, 78457 Konstanz, Germany

[$] Current address: UMR6112 'LPGN', CNRS / Université de Nantes, Faculté des Sciences et Techniques, 2 rue de la Houssinière, BP 92208, 44322 Nantes cedex 3, France.

Running title: Photoprotection in intertidal benthic diatoms

Keywords: benthic / diatom / intertidal flat / non-photochemical quenching / photoprotection / xanthophyll

Subject category: Microbial ecology and functional diversity of natural habitats

Abstract

In intertidal marine sediments, characterized by rapidly fluctuating and often extreme light conditions, primary production is frequently dominated by diatoms. We performed a comparative analysis of photophysiological traits in 15 marine benthic diatom species belonging to the four major morphological growth forms (epipelon, motile and non-motile epipsammon and tychoplankton) found in these sediments. Our analyses revealed a clear relationship between growth form and photoprotective capacity, and identified fast regulatory physiological photoprotective traits (i.e. non-photochemical quenching and the xanthophyll cycle) as key traits defining the functional light response of these diatoms. Non-motile epipsammon and motile epipelon showed the highest and lowest non-photochemical quenching respectively, with motile epipsammon showing intermediate values. Like epipelon, tychoplankton had low non-photochemical quenching, irrespective of whether they were grown in benthic or planktonic conditions, reflecting an adaptation to a low light environment. Our results thus provide the first experimental evidence for the existence of a trade-off between behavioural (motility) and physiological photoprotective mechanisms (non-photochemical quenching and the xanthophyll cycle) in the four major intertidal benthic diatoms growth forms using unialgal cultures. Remarkably, while motility is restricted to the raphid pennate diatom clade, raphid pennate species which have adopted a non-motile epipsammic or a tychoplanktonic life style display the physiological photoprotective response typical of these growth forms. This observation underscores the importance of growth form and not phylogenetic relatedness as the prime determinant shaping the physiological photoprotective capacity of benthic diatoms.

Introduction

Functional trait-based approaches are increasingly adopted to explain and understand the distribution and diversity of phytoplankton communities (Litchman and Klausmeier, 2008; Barton e*t al.*, 2013; Edwards e*t al.*, 2013). Various morphological and physiological traits have been shown to define the ecological niches of phytoplankton species, including size, temperature response and resource acquisition and utilization traits. For example, in planktonic diatoms, which play a key role in marine primary production and biogeochemical cycling (Armbrust, 2009), pronounced species-specific differences in photosynthetic architecture and photophysiological strategies have been documented (e.g. Dimier e*t al.*, 2007; Key e*t al.*, 2010; Schwaderer e*t al.*, 2011; Wu e*t al.*, 2012) and related to their *in situ* light environment (Strzepek and Harrison, 2004; Lavaud e*t al.*, 2007; Dimier e*t al.*, 2009; Petrou e*t al.*, 2011). A high capacity for physiological photoprotection is generally observed in highly fluctuating light climates and/or under on average high irradiances. This suggests that photoprotective capacity is an adaptive trait that shapes the distribution of planktonic diatoms in the environment (Lavaud e*t al.*, 2007; Dimier e*t al.*, 2009; Bailleul e*t al.*, 2010; Petrou e*t al.*, 2011; Lavaud and Lepetit, 2013).

Benthic marine environments, and especially intertidal environments, are characterized by even more changeable and extreme light climates resulting from the interplay of weather conditions, tides, water column turbidity and sediment composition (and hence light penetration) (Admiraal, 1984; Underwood and Kromkamp, 1999; Paterson and Hagerthey, 2001). Nevertheless, intertidal sediments rank amongst the most productive ecosystems on Earth, largely owing to the primary production of highly diverse assemblages of benthic diatoms (Underwood and Kromkamp, 1999). To date however, little is known about the role of functional traits, and especially photophysiological traits, in shaping the structure, dynamics and function of benthic diatom assemblages. In most studies, diatom functional groups are defined on the basis of morphological growth form (e.g. Gottschalk and Kahlert, 2012; Larson and Passy, 2012) and not physiological traits. In addition, photoprotective ability (limited to the measurement of the 'xanthophyll cycle', XC) and its relationship with ecology has only been studied in natural communities with mixed assemblages of functional groups (e.g. Jesus e*t al.*, 2009; van Leeuwe e*t al.*, 2009; Cartaxana e*t al.*, 2011).

In temperate seas, intertidal benthic communities are largely dominated by diatoms (Méléder e*t al.*, 2007; Ribeiro e*t al.*, 2013), which display a high degree of taxonomic, phylogenetic and functional diversity (Kooistra *et al.*, 2007). Several growth forms can be distinguished, which mainly differ in their attachment mode and degree of motility (see Ribeiro *et al.* (2013) for a detailed description): (1) the epipelon (EPL) comprises larger (usually > 10 µm) motile diatoms which can move freely in between sediment particles and typically form biofilms (cf. (Herlory e*t al.*, 2004); (2) the epipsammon (EPM) groups smaller (usually < 10 µm) diatoms which live in close association with individual sand grains; and (3) the tychoplankton (TYCHO), which is an ill-defined and rather enigmatic group of largely non-motile diatoms which presumably have an amphibious life style (both sediment and water column) (e.g. Sabbe *et al.* (2010)). Within the epipsammic group, non-motile (EPM-NM) species are firmly attached (either stalked or adnate) to sand particles, while motile forms (EPM-M) can move within the sphere of individual sand grains. From a phylogenetic perspective, motile forms (i.e. all epipelon and motile epipsammon) exclusively belong to the pennate raphid clade (Kooistra *et al.*, 2007), possessing a raphe allowing motility. Most non-motile epipsammon belongs to the pennate araphid lineage, but also includes some raphid pennates, such as *Biremis lucens*, which firmly attaches to sand grains (Sabbe e*t al.*, 1995). Tychoplankton includes both centric and pennate raphid forms. Intertidal benthic diatom species, but also growth forms, show distinct distribution patterns in time and space, suggesting pronounced (micro)niche differentiation (Sabbe, 1993; Méléder *et al.*, 2007, Ribeiro e*t al.*, 2013). For example, epipsammon dominates non-cohesive sandy sediments (Méléder *et al.*, 2007), while epipelon dominates cohesive muddy sediments (Haubois *et al.*, 2005). Epipelon typically display vertical 'micromigration' in the sediment following endogenous tidal/dial rhythms and environmental stimuli (Saburova and Polikarpov, 2003; Consalvey *et al.*, 2004; Coelho e*t al.*, 2011): during daylight emersion, they migrate to the sediment surface, while during immersion they migrate to deeper sediment layers.

To prevent photoinhibition (Serôdio e*t al.*, 2008), benthic diatoms utilize behavioural and physiological responses (Mouget e*t al.*, 2008; van Leeuwe e*t al.*, 2009; Perkins e*t al.*, 2010b; Cartaxana e*t al.*, 2011; Serôdio e*t al.*, 2012). Behavioural photoprotection involves motility, allowing cells to position themselves in light gradients and escape from prolonged exposure to excess light (Admiraal, 1984; Kromkamp e*t al.*, 1998; Consalvey e*t al.*, 2004; Serôdio *et al.*, 2006). In addition, both motile and non-motile species employ fast regulatory physiological processes for photoprotection (i.e. 'physiological photoprotection'; Lavaud, 2007; Goss and Jakob, 2010; Depauw e*t al.*, 2012; Lepetit e*t al.*, 2012). In diatoms, two processes are important in field situations (Lavaud, 2007): photosystem II cyclic electron transfer (PSII CET) and non-photochemical quenching of chlorophyll (Chl) fluorescence (NPQ) (Depauw e*t al.*, 2012; Lepetit e*t al.*, 2012; Lavaud and Lepetit, 2013). NPQ is controlled by several regulatory partners including the light-dependent conversion of diadinoxanthin (DD) to diatoxanthin (DT) by the DD de-epoxidase (i.e. the XC) (Brunet and Lavaud, 2010; Goss and Jakob, 2010). In benthic diatoms however, XC-NPQ has only rarely been studied, and mostly *in situ*: it has been shown to vary with diurnal and tidal cycles, season, latitude (Serôdio e*t al.*, 2005; van Leeuwe e*t al.*, 2009; Chevalier e*t al.*, 2010), the organisms' position within the sediments and along the intertidal elevation gradient (Jesus e*t al.*, 2009; Cartaxana e*t al.*, 2011). On the basis of their *in situ* measurements, the latter authors hypothesized the existence of a trade-off between behavioural and physiological photoprotection mechanisms in benthic diatoms as a stronger XC was shown to occur in sandy *vs.* muddy sediments. However, at least the sandy sediments contained a mix of both epipsammic and epipelic forms (Jesus e*t al.*, 2009; Cartaxana e*t al.*, 2011), and even when the latter are not numerically dominant, they can still make a substantial contribution to biomass due to their much larger biovolumes (see e.g. Hamels *et al*. 1998).

Our study represents a comprehensive characterization of fast regulatory physiological photoprotection capacity in typical representatives of the major diatom growth forms occurring in intertidal marine sediments. Given the highly dynamic and often extreme intertidal light climate, we hypothesize that photoprotective features are key traits shaping niche differentiation between benthic growth forms, as has been proposed before for phytoplankton (Huisman e*t al.*, 2001; Litchman and Klausmeier, 2008; Dimier e*t al.*, 2009; Petrou e*t al.*, 2011; Lavaud and Lepetit, 2013). In this respect, we predict that the largely immotile epipsammic life forms are better able to cope with pronounced and rapid changes in light intensity at the physiological level than the motile epipelic forms which can actively position themselves in the sediment light gradient.

Materials and methods

Diatom culturing and harvesting (Table 1)

Fifteen benthic diatom strains were used (Table 1). All species were assigned to their respective growth form on the basis of microscopical observations on natural assemblages. They were grown in batch cultures at 20°C in sterile artificial F/2 seawater medium enriched with $NaHCO_3$ (80 mg L^{-1} final concentration). Tychoplankton species were also grown in continuously flushed airlift (i.e. with air bubbling) to mimic 'planktonic' growth conditions. Two light intensities (E, 20 and 75 µmol photons m^{-2} s^{-1}) were used with a 16 h light:8 h dark photoperiod white fluorescent tubes, L58W/840, OSRAM, Germany. Cultures were photoacclimated to the above conditions at least 2 weeks before measurements and experiments (see below). Diatom suspensions for the experiments were prepared to a final concentration of 10 µg chlorophyll *a* (Chl *a*) mL^{-1}. For this purpose, Chl *a* concentration was determined according to the (Jeffrey and Humphrey, 1975) spectrophotometric method. Diatoms suspensions were continuously stirred at 20°C under the growth E (i.e. 20 or 75 µmol photons m^{-2} s^{-1}) at least 1 h before the start of the experiments and all along the course of the experiments (Lavaud e*t al.*, 2007). This kept the photosynthetic machinery in an oxidized state and prevented NPQ.

Growth rates and biovolumes

Specific growth rates, µ (d^{-1}), were calculated from regression of the natural logarithm of the number of diatom cells during their exponential growth phase as microscopically determined in a Malassez's counting chamber. Biovolumes (µm^3) were calculated using the formula of (Hillebrand e*t al.*, 1999) based on measurements performed on fifteen specimens per species.

HPLC pigment analyses

Chl *a*, Chlorophyll *c* (Chl *c*), fucoxanthin (Fx), DD, DT and ß-carotene (ß-car) content, all normalized to Chl *a* (i.e. expressed as mol. 100 mol Chl a^{-1}), were measured using HPLC as described in Jakob e*t al.* (1999). 1 mL of diatom suspension was rapidly filtered (Isopore 1.2 µm RTTP filters, Merck Millipore, Ireland) and immediately frozen in liquid nitrogen before extraction in a cold (4°C) mixture of 90% methanol/0.2 M ammonium acetate (90/10 vol/vol) and 10% ethyl acetate. The pigment extraction was improved by the use of glass beads (diameter 0.25-0.5 mm, Roth, Germany) and included several short (20 s) vortexing steps. Supernatants were collected after centrifugation (5 min, 10 000 g, 4°C) and immediately injected into an HPLC system (Hitachi Lachrom Elite, Japan) equipped with a cooled auto-sampler and a photodiode array detector (L-2455). Chromatographic separation was carried out using a Nucleosil 120-5 C18 column (125 mm long, 4 mm internal diameter, 5 µm particles, Macherey-Nagel, Germany) equipped with a pre-column (CC 8/4 Nucleosil, Macherey-Nagel, Germany) for reverse phase chromatography during a 25 min elution program. The solvent gradient followed Jakob et al. (1999) with an injection volume of 50 µL and a flow rate of 1.5 mL min^{-1}. Pigments were identified from absorbance spectra (400-800 nm) and retention times (Roy *et al*., 2011), and their concentrations were obtained from the signals in the photodiode array detector at 440 nm. The de-epoxidation state (DES in %) was calculated as [(DT / DD + DT) x 100], where DD is the epoxidized form and DT is the de-epoxidized form. Chl *a* concentration per cell was determined during exponential growth based on cell counts (see above) and the Chl *a* measurements.

Chl fluorescence yield and light curves (Table 2)

For a complete overview of the definition and measurement of the photophysiological parameters, see Table 2. Chl fluorescence yield was monitored with a Diving-PAM fluorometer (Walz, Germany) on a 2.5 mL stirred and 20°C controlled diatom suspension (Lavaud et al 2004). Before measurement, the cells were dark-adapted for 15 min, and a saturating pulse (3600 µmol photons m^{-2} s^{-1}, duration 0.4 ms) was fired to measure F_0, Fm and F_v/F_m. Two types of light curves were performed: Non Sequential and Rapid Light Curves (NSLCs and RLCs) (Perkins e*t al.*, 2010a). For NSLCs, continuous light (KL-2500 lamp, Schott, Germany) was applied for 5 min at different Es (48-1950 µmol photons.m^{-2}.s^{-1}); a new diatom suspension was used for each E. At the end of each exposure, F_m' and NPQ were measured. For RLCs, one diatom suspension was exposed to 8 successive, incrementally increasing Es (29-1042 µmol photons.m^{-2}.s^{-1}) of 30 s each (Perkins e*t al.*, 2006) (Table S1). RLCs allow constructing rETR *vs*. E and NPQ *vs*. E curves. The NPQ *vs*. E curve is based on a 3-parameter Hill equation model and it is described by the equation NPQ (E) = NPQ_m x $[E^{nNPQ}/(E50_{NPQ}{}^{nNPQ} + E^{nNPQ}$')] (Serôdio and Lavaud, 2011). From the fitted rETR-E curves (Eilers and Peeters, 1988) and NPQ-E curves (Serôdio and Lavaud, 2011), $rETR_m$, α, E_k, and NPQ_m, $E50_{NPQ}$, n_{NPQ} can be derived, respectively. All parameters are described in the Table 2. n_{NPQ} is the Hill coefficient or the sigmoidicity coefficient of the NPQ-E curve (Serôdio and Lavaud, 2011). It informs on the onset of NPQ at moderate Es, i.e. when the DT molecules are being 'activated' with increasing Es to effectively participate to NPQ: DT 'activation' depends on its enzymatic conversion and its binding to the PSII light-harvesting antenna complex in order to promote the antenna switch to a dissipative state of excess energy which is measurable by NPQ (see Lavaud and Lepetit, 2013). When n_{NPQ} is < 1, the NPQ-E curve shows an asymptotic saturation-like increase towards NPQ_m, while when n_{NPQ} is > 1, the NPQ-E curve shows a sigmoidal shape. In the later case, the Hill reaction (i.e. NPQ onset) is allosteric (as proposed for the NPQ mechanism, see Lavaud and Lepetit, 2013), n_{NPQ} thus informing on the degree of allostery of the NPQ-E curve. The higher n_{NPQ}, the more positively cooperative the Hill reaction is; n_{NPQ} around 2 being the highest values reported so far (Serôdio and Lavaud, 2011). The same fitting procedure can obviously be used for the DT-E and the DES-E curves, thereby extracting analogous parameters as from the fitted NPQ-E curves.

O_2 yield and the PSII CET

The relative O_2 yield produced during a sequence of single-turnover saturating flashes at a frequency of 2 Hz was measured with a home-made rate electrode (Lavaud e*t al.*, 2002). The steady-state O_2 yield per flash (Y_{SS}) was attained for the last 4 flashes of a sequence of 20 when the S-state cycle oscillations were fully damped (Lavaud e*t al.*, 2002). Y_{SS} of 15 min dark-adapted ($_{\mathbf{D}}$) and illuminated ($_{\mathbf{L}}$, samples taken at the end of each NSLC) cells was used to calculate the PSII CET (Lavaud e*t al.*, 2002; Lavaud e*t al.*, 2007) as follows: $[\{(20 \mathrm{x} Y_{SS\ \mathbf{L}})-(\Sigma (Y_{1\ldots 20})_{\mathbf{L}})\} - \{(20 \mathrm{x} Y_{SS\ \mathbf{D}})-(\Sigma (Y_{1\ldots 20})_{\mathbf{D}})\}] / Y_{SS\ \mathbf{D}}$.

Statistics

Statistical analyses were conducted using the statistical software package SAS 9.3. Species were compared using the general linear model PROC GLM. Growth forms (groups) were compared using the mixed linear model PROC MIXED. Groups were regarded as fixed effects. Data were log- or square root-transformed when needed to allow the best possible fit. Where necessary, estimated least squares means (lsmeans) and standard errors (SE) were back-transformed as in Jørgensen and Pedersen (1998).

Results

Growth rate and photosynthetic properties (Fig. S1, Tables 3, S2, S3)

The Chl *a* concentration per cell showed an exponential relationship with biovolume with relatively small changes at the smaller cell volumes (Fig. S1) The average diatom biovolumes were independent of growth form (Table 3, Fig. S1). Growth rate did not differ significantly between the growth forms at growth E = 20 µmol photons m^{-2} s^{-1}. Relative concentrations of the light-harvesting pigments Chl *c* and Fx were comparable among growth forms. ß-car, which is mainly associated with the photosystem cores, was only slightly but significantly higher in epipelon than in non-motile epipsammon. DD+DT content was significantly lower in epipelon than in the other growth forms. Because the cells were grown at low E, DES was generally low, with no significant differences between the growth forms. The highest DD+DT (16.95 ± 2.56 mol 100 mol Chl a^{-1}) and DES (16.4 ± 6.2 %) values were observed in *Plagiogramma staurophorum* (non-motile epipsammon). There were no significant differences in F_v/F_m, α, $rETR_{m,}$ E_k and PSII CET_{max} between the growth forms. E_k was on average 3 to 4 times the growth E in all growth forms. PSII CET_m was close to 3 (its maximum, Lavaud e*t al.*, 2002) for the two epipsammon growth forms, and about 2 in epipelon and tychoplankton.

NPQ properties (Figs 1, S2, Tables 4, S4-S6)

At E values ≥ 230 µmol photons m^{-2} s^{-1}, NPQ was significantly higher in non-motile epipsammon than in both epipelon and tychoplankton; the same holds true for motile epipsammon vs. epipelon and tychoplankton at E values ≥ 1050 µmol photons m^{-2} s^{-1}. NPQ was also significantly higher in non-motile epipsammon than in motile epipsammon except at the lowest and highest E values. Likewise, NPQ_m was significantly higher (x 3.5 and x 2.4, respectively) in non-motile epipsammon and motile epipsammon than in epipelon and tychoplankton. In epipelon and tychoplankton, the NPQ-E curves showed a lower variability than in the two epipsammon growth forms. Non-motile epipsammon had the lowest $E50_{NPQ}$, significantly lower than all other groups. In contrast, tychoplankton $E50_{NPQ}$ was significantly higher than in the other groups. Epipelic and motile epipsammic $E50_{NPQ}$ did not differ significantly from each other. In contrast, n_{NPQ} was not significantly different and varied around its optimum (i.e. 2, Serôdio and Lavaud, 2011) in most species except the tychoplanktonic ones (which is significantly lower than in epipsammon non-motile).

XC properties (Figs 1-2, Tables 4, S4, S6, S7)

DES was only significantly different between epipelon and both tychoplankton and motile epipsammon at 105 µmol photons.$m^{-2}.s^{-1}$ and between epipelon and both epipsammic forms at 230 µmol photons.$m^{-2}.s^{-1}$. DES_m varied between 21.2 ± 3.4 for epipelon, 22.7 ± 4.4 for tychoplankton, 28.7 ± 4.4 for motile epipsammon-M and 29.4 ± 3.8 for non-motile epipsammon (lsmeans ± SE). The slight difference between epipelon and the epipsammon growth forms, although not significant, in combination with the significantly higher DD+DT in the latter, generated a significantly lower DT_m in epipelon than in the epipsammon growth forms. $E50_{DT}$ was close to the $E50_{NPQ}$ in all growth forms except in tychoplankton where it was lower; no significant differences between the epipsammon and epipelon were observed, only non-motile epipsammon and tychoplankton $E50_{DT}$ differed significantly. n_{DT} was significantly lower in motile epipsammon and tychoplankton than in epipelon and non-motile epipsammon. NPQ/DT was about half its optimum (= 1 under these experimental conditions) in all groups except non-motile epipsammon. It roughly followed the same order as observed for NPQ_m, i.e. non-motile epipsammon > motile epipsammon > epipelon ≅ tychoplankton, with a 2x higher value in non-motile epipsammon. The difference between non-motile epipsammon and the other growth forms, however, was not significant due to the low

NPQ/DT value in *Plagiogramma staurophorum*. Fig 2 shows that in all growth forms except motile epipsammon there were species (*Seminavis robusta, Fragilaria.* cf. *subsalina, P. staurophorum*, *Brockmanniella brockmannii*) for which a low NPQ developed without DT synthesis, while two motile epipsammon species (*Amphora* sp. and *Planothidium delicatulum*) showed DT synthesis (0.17 ± 0.03 mol 100 mol Chl a^{-1}) without NPQ. All other species showed a NPQ/DT relationship with an origin close to 0, as expected.

Effect of high light acclimation on the NPQ and XC properties (Figs 3-4, Tables S8-S9)

All species were grown under an E (75 µmol photons m^{-2} s^{-1}) roughly corresponding to the mean E_k for the low E acclimated cells (20 µmol photons m^{-2} s^{-1}, Table 3). Only epipelon had significantly higher growth rates at 75 µmol photons m^{-2} s^{-1}. DD+DT significantly increased with a factor 1.6-1.7 in epipelon and epipsammon, and 2.3 in tychoplankton. There was a significant increase in DES at 75 µmol photons m^{-2} s^{-1} in all growth forms except in motile epipsammon. The increase in DD+DT and DES at the higher light intensity was most pronounced in tychoplankton and resulted in a pronounced, significant difference in both parameters between tychoplankton and epipelon at this light intensity. The comparison of Chl fluorescence yield and light curve parameters could only be performed for a selection of six species (covering all growth forms) and is summarised in Fig. 4. As expected, the Chl *a* content per cell decreased, roughly with a factor of 2 in all species (except *Navicula phyllepta*). There was only a slight (up to about 10 %) decrease in F_v/F_m in all species, illustrating the unstressed state of the cells (note that in *Seminavis robusta* and *Planothidium delicatulum* this decrease was slightly significant). DES_m significantly increased in *S. robusta* only. Together with the overall increase in DD+DT, this resulted in a significant increase in DT_m (by a factor of 4) in this species, but also in *P. delicatulum* and *Plagiogrammopsis vanheurckii*. The corresponding NPQ_m did not follow the same trend: it significantly increased in all species (except for *P. delicatulum* and *Opephora* sp.) but only by a factor of maximally 2. NPQ/DT remained low (0.2 to 0.5) in all species (and significantly decreased in *Opephora* sp.). $E50_{NPQ}$ was significantly higher only in the non-motile epipsammic species *Plagiogramma staurophorum*.

Effect of 'planktonic' growth on the NPQ and XC properties of tychoplankton (Fig. 5, Table S10)

The three tychoplanktonic species were grown under 'planktonic' conditions (at 20 µmol photons.$m^{-2}.s^{-1}$) for a comparison with growth under 'benthic' conditions. *Brockmaniella brockmannii* responded most strongly to a switch from 'benthic' to 'planktonic' growth: it showed a significantly lower growth rate and a higher DES and DES_m but a lower NPQ_m, suggesting photosynthetic stress and investment of additional DT in other processes than NPQ. *Plagiogrammopsis vanheurckii* and *Cylindrotheca closterium* showed very little change, apart from a significantly higher growth rate during planktonic growth in *P. vanheurckii*, a slight decrease in NPQ/DT in *C. closterium*, and an increase in DES in both species. The most pronounced and consistent change in tychoplankton thus concerned an increase in DES when grown in suspension. Note that there is also an overall decrease in $rETR_m$, but this decrease was just not significant (p=0.08).

Discussion

The present work constitutes the first comparative experimental study, using unialgal cultures in standardized conditions, of fast regulatory photoprotective mechanisms in the four main benthic diatom growth forms present in intertidal marine sediments (epipelon, motile and non-motile epipsammon and tychoplankton). Because no sediment was added in our experiments, motile diatoms were not able to position themselves in a light gradient, hence effectively incapacitating their behavioural response. As the growth rate and photosynthetic characteristics (main pigments, F_v/F_m, α, E_k, $rETR_m$) of the studied species were comparable between the growth forms at 20 µmol photons m^{-2} s^{-1}, we were able to compare their purely physiological light response.

Our study revealed a highly significant and pronounced difference in NPQ between the four growth forms. NPQ was significantly lower in epipelic and tychoplanktonic than in epipsammic species; differences in DES were only observed between epipelic and other forms at lower light intensities. Within the epipsammon, NPQ capacity was significantly higher in the non-motile than in the motile forms. As all growth forms included both small and large species, the functional light response (NPQ capacity) apparently did not depend on biovolume or the Chl *a* concentration per cell, as has also been observed *in situ* (Jesus e*t al.*, 2009). The absence of significant differences in PSII CET between growth forms underscores the importance of NPQ as the main fast photoprotective process in intertidal benthic diatoms, confirming earlier results for these organisms (Lavaud *et al.*, 2002) but in contrast with planktonic diatoms (Lavaud e*t al.*, 2002; Lavaud e*t al.*, 2007). By analogy with previous studies on planktonic diatoms (Dimier e*t al.*, 2009; Lavaud e*t al.*, 2007; Lavaud and Lepetit, 2013; Petrou e*t al.*, 2011; Strzepek and Harrison, 2004), our data suggest that epipelic and tychoplanktonic diatoms are adapted to a less fluctuating light climate and/or to a lower average irradiance, and vice versa for epipsammic diatoms. This result fits well with the ecology of these growth forms. Epipelon is not only more abundant in muddy cohesive sediments where light penetration is more restricted than in sandy sediments (Paterson and Hagerthey 2001; Cartaxana e*t al.*, 2011), but, more importantly, their (micro-)migratory behaviour allows positioning at the optimal irradiance in the vertical light gradient and rapid escape from periodic excess light (Kromkamp e*t al.*, 1998; Conn e*t al.*, 2004; Consalvey e*t al.*, 2004; Serôdio e*t al.*, 2006). This alleviates the need to invest in a strong physiological capacity to respond to light stress as previously proposed (Jesus e*t al.*, 2009; Cartaxana e*t al.*, 2011), although the right balance between motility and physiology still remains essential (van Leeuwe e*t al.*, 2009; Perkins e*t al.*, 2010b; Cartaxana e*t al.*, 2011; Serôdio e*t al.*, 2012).

Such balance is more crucial in the motile epipsammic species, which can move but have only limited control over their immediate light environment as movement is restricted, usually within the sphere of individual sand grains. As expected, they showed a significantly lower NPQ and a higher $E50_{NPQ}$ than non-motile epipsammon, which have no behavioural control over their light environment. An alternative, but not exclusive, explanation could be related to the difference in exopolysaccharide (EPS) secretion between motile and non-motile growth forms. EPS secretion could work as an alternative electron sink under stressful conditions (i.e. high light, nutrient limitation, etc.) in order to limit the over-reduction of the photosynthetic machinery (‘overflow’ hypothesis; Staats et al., 2000), alleviating the need for a strong NPQ. However, EPS secretion is not as fast as NPQ (minutes/hours *vs*. seconds/minutes) and may not be useful to the cells for responding to rapid light changes but only to cope with prolonged high light exposure. Additionally, while the ‘overflow’ hypothesis is often proposed (Underwood and Paterson, 2003; Stal, 2009), it was never clearly proven. A few studies have shown a positive relationship between light intensity and EPS production

(Underwood, 2002; Wolfstein and Stal, 2002) but other studies have reported a negative relation with light intensity and no relationship with nutrient limitation (Hanlon e*t al*., 2001; Perkins *et al*., 2006). To date there is no information on EPS production in different benthic diatom growth forms, and only epipelic species have been compared (Underwood and Paterson, 2003), showing no clear relationship between light response and EPS secretion. To our knowledge, there are no reports on a relationship between NPQ-XC capacity and EPS production. Finally, tychoplankton typically alternates between resuspension in a highly turbid shallow water column at high tide and deposition and burial in the upper sediment layers of muddy sediments at low tide (deposition in sandy sediments does not occur due to the intense hydrodynamic disturbance in these sediments). As such, the tychoplankton resembles planktonic diatoms adapted to subtle light fluctuations and/or on average low irradiance (Bailleul e*t al*., 2010; Lavaud and Lepetit, 2013).

The reason for the NPQ differences between epipelon and epipsammon can be explained by its main control: the XC dynamics. Previous *in situ* studies reported a consistently stronger DES under light stress in epipsammic than in epipelic diatom communities (i.e. in sandy *vs*. muddy sediments) and related growth form with differential (behavioural *vs*. physiological) photoregulatory strategies (Jesus e*t al*., 2009; Cartaxana e*t al*., 2011). As recently shown, a high NPQ is supported by the strong effective involvement of DT which first depends both on a high DD+DT content and a high DES (Lavaud and Lepetit, 2013). The slope of the NPQ/DT relationship has been proposed as a good indicator of light climate adaptation: the higher the NPQ/DT slope, the better the adaptation to a highly fluctuating and/or on average high light climate (Dimier e*t al*., 2009; Lavaud and Lepetit, 2013). All epipsammic species, and especially the non-motile ones, showed XC parameter values which are characteristic for a high NPQ capacity, viz. a higher DD+DT content and DT_m which was 2x higher than in epipelon. Non-motile epipsammon also tended to show a higher efficiency in promoting NPQ (NPQ/DT), but this difference was not significant due to high intra-group variability.

Within the epipsammon, NPQ is clearly more efficient in non-motile than motile epipsammic species. In motile epipsammon, the discrepancy between $E50_{NPQ}$ and E_k is more pronounced than in non-motile forms: while there is no significant difference in E_k between both growth forms, $E50_{NPQ}$ is significantly higher in the motile growth forms. This suggests a weaker relationship between NPQ development and photochemistry in the latter group, with slower NPQ development with increasing E. Remarkably, $E50_{DT}$ does not significantly differ between both growth forms, and the significantly higher initial induction of DT synthesis (n_{DT}) but not NPQ (n_{NPQ}) in the motile group, together with the fact that some representatives of this group show DT synthesis without NPQ, suggests that either DT is less or not involved in NPQ development, or that the light-dependent built-up of the transthylakoidal proton gradient (which is involved in both the activation of the DD de-epoxidase and the molecular control of NPQ) and the onset of NPQ are uncoupled (Lavaud e*t al.*, 2012; Lavaud and Lepetit, 2013). Our observations thus suggest that in contrast to the non-motile group, motile epipsammic species rely more on a behavioural response (motility) and/or involve DT in other photoprotective processes such as the prevention of lipid peroxidation by reactive oxygen species (ROS) (Lepetit e*t al.*, 2010). The increase in $E50_{NPQ}$ in the non-motile epipsammic species *Plagiogramma staurophorum* during a shift to higher light illustrates the ability to physiologically modulate the NPQ *vs*. E development kinetics to its light environment in contrast to motile epipsammon, epipelon and tychoplankton.

The influence of DT on the inter-group/species NPQ differences was further investigated by the acclimation to higher light (75 µmol photons m^{-2} s^{-1}, close to the mean E_k for cells acclimated to 20 µmol photons m^{-2} s^{-1}). High light exposure is known to induce constitutive

DT synthesis (Schumann e*t al.*, 2007) and in field conditions, DT is usually even present in significant amounts in cells adapted to low/moderate light (Jesus e*t al.*, 2009; van Leeuwe *et al.*, 2009; Chevalier e*t al.*, 2010; Cartaxana e*t al.*, 2011). Acclimation to higher light resulted in a significant increase in XC pigments (DD+DT) and DES in most growth forms, suggesting that although epipelon uses behavioural photoprotection, the XC is still important (cf. above). NPQ_m increased in most of the species examined, mainly due to a higher DT_m resulting from a higher DD+DT rather than a higher DES_m. The discrepancy between DES_m and NPQ_m as well as the low NPQ/DT may be due to the fact that the additional DT primarily served in the prevention of lipid peroxidation rather than in NPQ as previously reported in high light acclimated diatoms (see also above).

While under low light conditions, the growth, photosynthetic and steady-state light-response features of tychoplankton were similar to those of epipelic diatoms (i.e. low NPQ, NPQ_m and DT_m), their dynamic light response was significantly different, i.e. higher $E50_{NPQ}$. Surprisingly, $E50_{NPQ}$ was beyond the natural light maximum (2000-2500 µmol photons m^{-2} s^{-1}) illustrating the inability of tychoplankton to strongly and/or continuously develop NPQ in the environmental high light range (a situation also encountered in one epipelic species: *Navicula phyllepta*). In contrast, its low n_{NPQ} supported a relatively strong onset of NPQ at low Es. Both $E50_{DT}$ and n_{DT} were correspondingly high and low, respectively (and significantly different from epipelon for n_{DT}), although $E50_{DT}$ was much lower than $E50_{NPQ}$ suggesting a discrepancy between DT synthesis and NPQ development (cf. above). The response of tychoplankton to higher light was much more pronounced, with the strongest increase in XC pigments and DES of all growth forms. However, the NPQ_m and DT_m data (only available however for one representative species, *Plagiogrammopsis vanheurckii*) did not show a similar response, with DT_m showing a more pronounced increase than NPQ_m, suggesting that NPQ development was low and that DT may have mainly been involved in other processes than NPQ. For most parameters, the response of the tychoplankton species to growth in suspension (‘planktonic’ growth) was limited and largely species-specific, except for a general increase in DES and a decrease (albeit just non-significant) in rETR$_m$. These data suggest that representatives of the tychoplanktonic growth form are well-adapted to their amphibious life style, which is characterized by an on average low irradiance (MacIntyre *et al.*, 1996). In contrast, epipelic species do not grow well in suspended, turbulent conditions (J. Lavaud, pers. observation).

Our study for the first time shows that intertidal benthic diatoms display growth form specific variation in fast regulatory physiological mechanisms for photoprotective capacity (NPQ and the XC), which mirrors their behavioural light response. In epipelic motile diatoms, exclusively belonging to the raphid pennate clade, the physiological response is not well developed, as these diatoms appear to largely rely on motility to control their immediate light environment. In the motile epipsammon however the physiological response remains essential because their movement is restricted to the sphere of individual sand grains. The evolution of the raphe system, the hallmark synapomorphy of the raphid pennate diatom clade which enables locomotion, has therefore been essential for the colonization of intertidal sediments by not only migratory epipelic biofilms but also motile epipsammon. In contrast, NPQ and XC capacity is high in non-motile araphid pennate diatoms which passively have to abide often pronounced variations in the intertidal light climate. Tychoplanktonic diatoms, which alternate between high tide resuspension in a turbulent and turbid water column, and low tide deposition in muddy sediments, appear to be adapted to an on average low light environment, with low NPQ and XC capacity.

While we made no formal analysis of the relationship between functional and phylogenetic diversity, it is obvious that despite the fact that a behavioural photoprotective response (motility) is restricted to the raphid pennate diatom clade, differences in the studied physiological traits are more strongly driven by growth form than phylogenetic relatedness. For example, the epipsammic species *Biremis lucens*, despite being a raphid pennate species, has a non-motile growth form, and shows a NPQ capacity which is more similar to non-motile epipsammon than to the (phylogenetically more closely related) motile epipsammon and epipelon. Likewise, photophysiological features of pennate raphid (*Cylindrotheca closterium*) and centric (*Plagiogrammopsis vanheurckii* and *Brockmanniella brockmannii*) tychoplankton species were similar as reported before in planktonic centric/pennate species (Lavaud *et al*., 2004). Raphid pennate diatoms which have colonized an epipsammic or tychoplanktonic niche thus display a reverse evolutionary trade-off switch towards a much more performant physiological response. Our observations thus suggest that photoprotective capacity in diatoms is a highly adaptive trait which is to a certain degree constrained by clade-specific evolutionary innovations (the evolution of the raphe system and hence a behavioural response) but also, and more importantly, by growth form, which ultimately defines the balance between the physiological and behavioural photoprotective response in these organisms. Such differential adaptation is of primary importance for the regulation of the photosynthetic productivity *vs*. light, as has been demonstrated before in planktonic diatoms, where the photochemical *vs*. the photoprotective energy allocation as a function of light is drastically different in species adapted to a fluctuating *vs*. a more stable light environment (Wagner *et al*., 2006; Lavaud *et al*., 2007; Petrou *et al*., 2011; Lavaud and Lepetit, 2013). However, unlike in planktonic environments, the trade-off between a physiological and behavioural response in benthic diatoms allows local co-existence of different growth forms under the same overall light environment.

Acknowledgements

The authors acknowledge the Centre National de la Recherche Scientifique-CNRS, the University of La Rochelle-ULR, the Contrat Plant Etat Région-CPER ‘Littoral’, the Region Poitou-Charentes, the Deutscher Akademischer Austausch Dienst-DAAD, the Research Foundation Flanders (FWO project G.0222.09N), Ghent University (BOF-GOA 01G01911) and the Egide/Campus France-PHC Tournesol (n°28992UA) exchange program for their financial support.

The authors formally declare that no conflict of interest exists.

Supplementary information is available at The ISME Journal’s website

References

Admiraal W. (1984). The ecology of estuarine sediment inhabiting diatoms. *Prog Phycol Res* **3:** 269-314.

Armbrust EV. (2009). The life of diatoms in the world's oceans. *Nature* **459:** 185-192.

Bailleul B, Rogato A, de Martino A, Coesel S, Cardol P, Bowler C *et al.* (2010). An atypical member of the light-harvesting complex stress-related protein family modulates diatom responses to light. *Proc Natl Acad Sci USA* **107:** 18214-18219.

Barton AD, Pershing AJ, Lichtman E, Record NR, Edwards KF, Finkel ZV *et al.* (2013). The biogeography of marine plankton traits. *Ecol Lett* **16:** 522-534.

Brunet C, Lavaud J. (2010). Can the xanthophyll cycle help extract the essence of the microalgal functional response to a variable light environment ? *J Plankton Res* **32:** 1609-1617.

Cartaxana P, Ruivo M, Hubas C, Davidson I, Serôdio J, Jesus B. (2011). Physiological versus behavioral photoprotection in intertidal epipelic and epipsammic benthic diatom communities. *J Exp Mar Biol Ecol* **405:** 120-127.

Chevalier EM, Gévaert F, Créach A. (2010). In situ photosynthetic activity and xanthophylls cycle development of undisturbed microphytobenthos in an intertidal mudflat. *J Exp Mar Biol Ecol* **385:** 44-49.

Coelho H, Vieira S, Serôdio J. (2011). Endogenous versus environmental control of vertical migration by intertidal benthic microalgae. *Eur J Phycol* **46:** 271-281.

Conn SA, Bahena M, Davis JT, Ragland RL, Rauschenberg CD, Smith BJ. (2004). Characterisation of the diatom photophobic response to high irradiance *Diatom Res* **19:** 167-179.

Consalvey M, Paterson DM, Underwood GJC. (2004). The ups and downs of life in a benthic biofilm: migration of benthic diatoms. *Diatom Res* **19:** 181-202.

Depauw FA, Rogato A, d'Alcala MR, Falciatore A. (2012). Exploring the molecular basis of responses to light in marine diatoms. *J Exp Bot* **63:** 1575-1591.

Dimier C, Corato F, Tramontano F, Brunet C. (2007). Photoprotective capacity as functional trait in planktonic algae: relationship between xanthophyll cycle and ecological characteristics in three diatoms. *J Phycol* **43:** 937-947.

Dimier C, Giovanni S, Ferdinando T, Brunet C. (2009). Comparative ecophysiology of the xanthophyll cycle in six marine phytoplanktonic species. *Protist* **160:** 397-411.

Edwards KF, Litchman E, Klausmeier CA. (2013). Functional traits explain phytoplankton community structure and seasonal dynamics in a marine ecosystem. *Ecol Lett* **16:** 56-63.

Eilers PHC, Peeters JCH. (1988). A model for the relationship between light intensity and the rate of photosynthesis in phytoplankton. *Ecol Model* **42:** 199-215.

Goss R, Jakob T. (2010). Regulation and function of xanthophyll cycle-dependent photoprotection in algae. *Photosynth Res* **106:** 103-122.

Gottschalk S, Kahlert M. (2012). Shifts in taxonomical and guild composition of littoral diatom assemblages along environmental gradients. *Hydrobiologia* **694:** 41-56.

Hamels I, Sabbe K, Muylaert K, Barranguet C, Lucas C, Herman P, Vyverman W. (1998) Organisation of microbenthic communities in intertidal estuarine flats, a case study from the Molenplaat (Westerschelde estuary, The Netherlands). *Europ J Protistol* **34:** 308-320.

Haubois A-G, Sylvestre F, Guarini J-M, Richard P, Blanchard GF. (2005). Spatio-temporal structure of the epipelic diatom assemblage from an intertidal mudflat in Marennes-Oleron Bay, France. *Est Coast Shelf Sci* **64:** 385-394.

Herlory O, Guarini J-M, Richard P, Blanchard GF. (2004). Microstructure of microphytobenthic biofilm and its spatio-temporal dynamics in an intertidal mudflat (Aiguillon Bay, France). *Mar Ecol Prog Ser* **282:** 33-44.

Hanlon ARM, Bellinger B, Haynes K, Xiao G, Hofmann TA, Gretz MR, Ball AS, Osborn AM, Underwood GJC. (2006) Dynamics of extracellular polymeric substance (EPS) production and loss in an estuarine, diatom-dominated, microalgal biofilm over a tidal emersion–immersion period. *Limnol Oceanogr* **51:** 79-93.

Hillebrand C, Durselen CD, Kirschtel D, Pollingher U, Zohary T. (1999). Biovolume calculation for pelagic and benthic microalgae. *J Phycol* **35:** 403-424.

Huisman J, Johansson AM, Folmer EO, Weissing FJ. (2001). Towards a solution of the plankton paradox: the importance of physiology and life history. *Ecol Lett* **4:** 408-411.

Jakob T, Goss R, Wilhelm C. (1999). Activation of diadinoxanthin de-epoxidase due to a chlororespiratory proton gradient in the dark in the diatom *Phaeodactylum tricornutum*. *Plant Biol* **1:** 76-82.

Jeffrey SW, Humphrey GR. (1975). New spectrophotometric equations for determining chlorophylls a, b, c1 and c2 in higher plants, algae and natural phytoplankton. *Biochem Physiol Pflanzen Bd* **167:** 191-194.

Jesus BM, Brotas V, Ribeiro L, Mendes CR, Cartaxana P, Paterson DM. (2009). Adaptations of microphytobenthos assemblages to sediment type and tidal position. *Cont Shelf Res* **29:** 1624-1634.

Jørgensen E, Pedersen AR. (1998). How to obtain those nasty standard errors from transformed data - and why they should not be used. In: 7 BRU-Ir (ed). Danish Institute of Agricultural Sciences. p 20.

Key T, McCarthy A, Campbell DA, Six C, Roy S, Finkel ZV. (2010). Cell size trade-offs govern light exploitation strategies in marine phytoplankton. *Environ Microbiol* **12:** 95-104.

Kooistra WHCF, Gersonde R, Medlin LK, Mann DG. (2007). The origin and the evolution of the diatoms: Their adaptation to a planktonic existence. In: Falkowski PG, Knoll AH (eds). *Evolution of Primary Producers in the Sea*. Elsevier Academic Press: Burlington. pp 207-249.

Kromkamp J, Barranguet C, Peene J. (1998). Determination of microphytobenthos PSII quantum efficiency and photosynthetic activity by means of variable chlorophyll fluorescence. *Mar Ecol Prog Ser* **162:** 45-55.

Larson CA, Passy SI. (2012). Taxonomic and functional composition of the algal benthos exhibits similar successional trends in response to nutrient supply and current velocity. *FEMS Microbiol Ecol* **80:** 352-360.

Lavaud J, van Gorkom HJ, Etienne A-L. (2002). Photosystem II electron transfer cycle and chlororespiration in planktonic diatoms. *Photosynth Res* **74:** 51-59.

Lavaud J, Rousseau B, Etienne A-L. (2004). General features of photoprotection by energy dissipation in planktonic diatoms (Bacillariophyceae). *J Phycol* **40:** 130-137.

Lavaud J (2007). Fast regulation of photosynthesis in diatoms: Mechanisms, evolution and ecophysiology. *Funct Plant Sci Biotech* **267:** 267-287.

Lavaud J, Strzepek RF, Kroth PG. (2007). Photoprotection capacity differs among diatoms: Possible consequences on the spatial distribution of diatoms related to fluctuations in the underwater light climate. *Limnol Oceanogr* **52:** 1188-1194.

Lavaud J, Materna AC, Sturm S, Vugrinec S, Kroth PG. (2012). Silencing of the violaxanthin de-epoxidase gene in the diatom *Phaeodactylum tricornutum* reduces diatoxanthin synthesis and non-photochemical quenching. *PLoS ONE* **7:** e36806.

Lavaud J, Lepetit B. (2013). An explanation for the inter-species variability of the photoprotective non-photochemical chlorophyll fluorescence quenching in diatoms. *Biochim Biophys Acta* **1827:** 294-302.

Lepetit B, Volke D, Gilbert M, Wilhelm C, Goss R. (2010). Evidence for the existence of one antenna-associated, lipid-dissolved and two protein-bound pools of diadinoxanthin cycle pigments in diatoms. *Plant Physiol* **154:** 1905-1920.

Lepetit B, Goss R, Jakob T, Wilhelm C. (2012). Molecular dynamics of the diatom thylakoid membrane under different light conditions. *Photosynth Res* **111:** 245-257.

Lepetit B, Sturm S, Rogato A, Gruber A, Sachse M, Falciatore A *et al.* (2013). High light acclimation in the secondary plastids containing diatom *Phaeodactylum tricornutum* is triggered by the redox state of the plastoquinone pool. *Plant Physiol* **161:** 853-865.

Litchman E, Klausmeier CA. (2008). Trait-based community ecology of phytoplankton. *Ann Rev Ecol Evol Syst* **39:** 615-639.

MacIntyre HL, Geider JR, Miller DC. (1996). Microphytobenthos: The ecological role of the 'secret garden' of unvegetated, shallow-water marine habitats. I. Distribution, abundance and primary production. *Estuaries* **19:** 186-201.

Méléder V, Rincé Y, Barillé L, Gaudin P, Rosa P. (2007). Spatiotemporal changes in microphytobenthos assemblages in a macrotidal flat (Bourgneuf Bay, France). *J Phycol* **43:** 1177-1190.

Mouget JL, Perkins R, Consalvey M, Lefebvre S. (2008). Migration or photoacclimation to prevent high irradiance and UV-B damage in marine microphytobenthic communities. *Aquat Microb. Ecol.* **52:** 223-232.

Paterson DM, Hagerthey SE. (2001). Microphytobenthos in contrasting coastal ecosystems: Biology and dynamics. In: Reise K. (ed). *Ecological Comparisons of Sedimentary Shores*. Springer-Verlag: Berlin Heidelberg. pp 106-125.

Perkins RG, Underwood GJC, Brotas V, Snow GC, Jesus B, Ribeiro L. (2001) Response of microphytobenthos to light: primary production and carbohydrate allocation over an emersion period. *Mar Ecol Prog Ser* **223:** 101-112.

Perkins RG, Mouget J-L, Lefebvre S, Lavaud J. (2006). Light response curve methodology and possible implications in the application of chlorophyll fluorescence to benthic diatoms. *Mar Biol* **149:** 703-712.

Perkins RG, Kromkamp JC, Serôdio J, Lavaud J, Jesus BM, Mouget J-L *et al.* (2010a). The Application of variable chlorophyll fluorescence to microphytobenthic biofilms. In: Suggett DJ, Prášil O, Borowitzka MA. (eds). *Chlorophyll a Fluorescence in Aquatic Sciences: Methods and Applications*. Springer Netherlands. pp 237-275.

Perkins RG, Lavaud J, Serôdio J, Mouget J-L, Cartaxana P, Rosa P *et al.* (2010b). Vertical cell movement is a primary response of intertidal benthic biofilms to increasing light dose. *Mar Ecol Prog Ser* **416:** 93-103.

Petrou K, Doblin MA, Ralph PJ. (2011). Heterogeneity in the photoprotective capacity of three Antarctic diatoms during short-term changes in salinity and temperature. *Mar Biol* **158:** 1029-1041.

Ribeiro L, Brotas V, Rincé Y, Jesus BM. (2013). Structure and diversity of intertidal benthic diatom assemblages in contrasting shores: A case study from the Tagus estuary. *J Phycol*.

Roy S, Llewellyn CA, Skarstad Egeland E, Johnsen G. (2011) Phytoplankton Pigments-Characterization, Chemotaxonomy and Applications in Oceanography, Cambridge Environmental Chemistry Series, Cambridge University Press, Cambridge, UK, 845 pp.

Underwood GJC. (2002). Adaptation of tropical marine microphytobenthic assemblages along a gradient for light and nutrient availability in Suva Lagoon, Fidji. *Eur J Phycol* **37:** 449-462.

Underwood GJC, Paterson DM. (2003). The importance of extracellular carbohydrate production by marine epiplelic diatoms. *Adv Bot Res* **40:** 183-240.

Sabbe K. (1993). Short-term fluctuations in benthic diatom numbers on an intertidal sandflat in the Westerschelde estuary (Zeeland, The Netherlands). *Hydrobiologia* **269-270:** 275-284.

Sabbe K, Witkowski A, Vyverman W. (1995). Taxonomy, morphology and ecology of *Biremis lucens* comb. nov. (Bacillariophyta): a brackish-marine, benthic diatom species comprising different morphological types. *Bot Mar* **38:** 379-391.

Sabbe K, Vanelslander B, Ribeiro L, Witkowski A, Muylaert K, Vyverman W. (2010). A new genus, *Pierrecomperia* gen. nov., a new species and two new combinations in the marine diatom family *Cymatosiraceae*. *Vie et Milieu* **60:** 243-256.

Saburova MA, Polikarpov IG. (2003). Diatom activity within soft sediments: behavioural and physiological processes. *Mar Ecol Prog Ser* **251:** 115-126.

Schumann A, Goss R, Jakob T, Wilhelm C. (2007). Investigation of the quenching efficiency of diatoxanthin in cells of *Phaeodactylum tricornutum* (Bacillariophyceae) with different pool sizes of xanthophyll cycle pigments. *Phycologia* **46:** 113-117.

Schwaderer AS, Yoshiyama K, de Tezanos Pinto P, Swenson NG, Klausmeier CA, Litchman E. (2011). Eco-evolutionary differences in light utilization traits and distributions of freshwater phytoplankton. *Limnol Oceanogr* **56:** 589-598.

Serôdio J, Cruz S, Vieira S, Brotas V. (2005). Non-photochemical quenching of chlorophyll fluorescence and operation of the xanthophyll cycle in estuarine microphytobenthos. *J Exp Mar Biol Ecol* **326:** 157-169.

Serôdio J, Coelho H, Vieira S, Cruz S. (2006). Microphytobenthos vertical migratory photoresponse as characterised by light-response curves of surface biomass. *Est Coast Shelf Sci* **68:** 547-556.

Serôdio J, Vieira S, Cruz S. (2008). Photosynthetic activity, photoprotection and photoinhibition in intertidal microphytobenthos as studied in situ using variable chlorophyll fluorescence. *Cont Shelf Res* **28:** 1363-1375.

Serôdio J, Lavaud J. (2011). A model for describing the light response of the nonphotochemical quenching of chlorophyll fluorescence. *Photosynth Res* **108:** 61-76.

Serôdio J, Ezequiel J, Barnett A, Mouget J-L, Méléder V, Laviale M *et al.* (2012). Efficiency of photoprotection in microphytobenthos: Role of vertical migration and the xanthophyll cycle against photoinhibition. *Aquat Microb Ecol* **67:** 161-175.

Staats N, Stal LJ, de Winder B., Mur LR. (2000). Oxygenic photosynthesis as driving process in exopolysaccharide production in benthic diatoms. *Mar Ecol Prog Ser* **193:** 261-269.

Stal LJ. (2009). Microphytobenthos as a biogeomorphological force in intertidal sediment stabilization. *Ecol Eng* **36:** 236-245.

Strzepek RF, Harrison PJ. (2004). Photosynthetic architecture differs in coastal and oceanic diatoms. *Nature* **431:** 689-692.

Underwood GJC, Kromkamp J. (1999). Primary production by phytoplankton and microphytobenthos in estuaries. In: Nedwell DB, Raffaelli DG. (eds). *Adv Ecol Res*. Academic Press. pp 93-153.

van Leeuwe MA, Brotas V, Consalvey M, Forster RM, Gillespie D, Jesus B *et al.* (2009). Photacclimation in microphytobenthos and the role of the xanthophylls pigments. *Eur J Phycol* **43:** 123-132.

Wagner H, Jakob T, Wilhelm C. (2006). Balancing the energy flow from captured light to biomass under fluctuating light conditions. *New Phytol* **169:** 95-108.

Wolstein K, Stal LJ. (2002). Production of extracellular polymeric substances (EPS) by bethic diatoms: effect of irradiance and temperature. *Mar Ecol Prog Ser* **236:** 13-22.

Wu H, Roy S, Alami M, Green BR, Campbell AD. (2012). Photosystem II photoinactivation, repair, and protection in marine centric diatoms. *Plant Physiol* **160:** 464-476.

Titles and legends to figures and tables.

Figure 1. Non-photochemical quenching of Chl fluorescence (NPQ) (A), de-epoxidation state of the diadinoxanthin (DD) to diatoxanthin (DT) [DES = DT / (DD + DT) x 100] (B), and DT content (C) as a function of light intensity (E from darkness to 1950 µmol photons m^{-2} s^{-1} which is equivalent to full sunlight in the field) measured during Non-Sequential Light Curves (NSLCs) in the four benthic diatom growth forms (EPM-NM, epipsammon non-motile, EPM-M, epipsammon motile; EPL, epipelon; TYCHO, thychoplankton). Cells were grown at 20 µmol photons m^{-2} s^{-1}. The NPQ-E curves for the individual species can be found in Fig. S2. Values are estimated least squares means ± estimated standard errors (PROC MIXED procedure).

Figure 2. Non-photochemical quenching of Chl fluorescence (NPQ) as a function of the amount of diatoxanthin (DT) measured during Non-Sequential Light Curves (NSLCs) in the five species of epipelon (EPL) (A), the four species of motile epipsammon (EPM-M) (B), the three species of tychoplankton (TYCHO) (C), and the three species of non-motile epipsammon (EPM-NM) (D). Cells were grown at 20 µmol photons m^{-2} s^{-1}. The full names and classification of all species is listed in Table 1.

Figure 3. Growth rate (µ) (A), diadinoxanthin (DD) + diatoxanthin (DT) content (B) and de-epoxidation state of DD to DT [DES = (DT / DD+DT x 100] (C) in the four benthic diatom growth forms (EPM-NM, epipsammon non-motile, EPM-M, epipsammon motile; EPL, epipelon motile; TYCHO, thychoplankton) for cells grown at light intensities of 20 and 75 µmol photons m^{-2} s^{-1} respectively. All parameters were measured on cells in exponential growth and sampled 2 h after the onset of light; growth conditions were 16 h light:8 h dark,

20°C. The values for all species in 20 and 75 µmol photons m^{-2} s^{-1} conditions are found in Tables S2 and S8, respectively. Values are estimated least squares means ± estimated standard errors (PROC MIXED procedure).

Figure 4. Comparison of photosynthetic, non-photochemical quenching of Chl fluorescence (NPQ) and xanthophyll cycle (XC) parameters measured in diatom species representative of the four benthic diatom growth forms grown at light intensities of 20 and 75 µmol photons m^{-2} s^{-1} respectively. For each parameter the ratio of the values obtained at 75 and 20 µmol photons m^{-2} s^{-1} – 1 was calculated (i.e. the 0 line is equal to a 75/20 ratio = 1 which is equivalent to no change of values between light intensities). Significant changes between both light intensities are indicated with an asterisk. The values used for the 20 and the 75 µmol photons m^{-2} s^{-1} conditions can be found in Tables S2/S4 and S8/S9 respectively.

Figure 5. Comparison of growth, photosynthetic, pigment, non-photochemical quenching of Chl fluorescence (NPQ) and xanthophyll cycle (XC) parameters measured in the three tychoplankton diatom species in ‘benthic’ and ‘planktonic’ conditions. For each parameter the ratio of the values obtained under benthic and planktonic conditions – 1 was calculated (i.e. the 0 line is equal to a planktonic/benthic ratio = 1 which is equivalent to no change of values between ‘benthic’ and ‘planktonic’ conditions). Chl *a* per cell (in pg cell-1) and growth rates (in day^{-1}) were measured on cells in exponential growth phase sampled 2 h after the onset of light; growth conditions were 20 µmol photons m^{-2} s^{-1}, 16 h light:8 h dark, 20°C. Significant changes between both light intensities are indicated with an asterisk. The values used for the ‘benthic’ and ‘planktonic’ growth conditions can be found in Tables S2/S4 and S10 respectively.

Table 1: List of the fifteen diatom species used in this study with their growth form classification, collection number, origin and average biovolume.

Abbreviations: NCC, Nantes Culture Collection-France ; UTCC, University of Toronto Culture Collection of Algae and Cyanobacteria-Canada (now the Canadian Phycological Culture Collection-CPCC); CCY, Culture Collection Yerseke-The Netherlands; DCG: BCCM (Belgian Coordinated Collections of Microorganisms) Diatom Culture Collection hosted by Laboratory for Protistology & Aquatic Ecology, Ghent University, Belgium ; n.d. not determined.

Table 2: Photophysiological parameters used in this study, their photophysiological meaning and measurement method and conditions. Abbreviations: Chl, chlorophyll; DD, diadinoxanthin; DT, diatoxanthin; E, light intensity; NSLCs, Non-Sequential Light Curves; PSII, photosystem II; RLCs, Rapid Light Curves. See the Materials and Methods section for further details.

Table 3: Growth rate, pigment content and photosynthetic properties of the four growth forms of benthic diatoms. All parameters were measured on cells in exponential growth phase sampled 2 h after the onset of light. Growth conditions were 20 µmol photons m^{-2} s^{-1}, 16 h light:8 h dark, 20°C. Abbreviations: EPL, epipelon; EPM-M, motile epipsammon; EPM-NM, non-motile epipsammon; TYCHO, tychoplankton. µ, growth rate (day^{-1}); Chl *a* $cell^{-1}$, content of chlorophyll *a* (in pg) per diatom cell; other pigments are expressed in mol 100 mol. Chl a^{-1}: Chl, chlorophyll; Fx, fucoxanthin; β-car, β-carotene; DD, diadinoxanthin; DT, diatoxanthin. Definitions and conditions of measurement of all parameters are listed in Table

2. The values for the individual species can be found in Table S2. Values are least squares means estimates and estimated standard errors (PROC MIXED procedure).

Table 4: Non-photochemical quenching (NPQ) and xanthophyll cycle (XC) properties of the four growth forms of benthic diatoms. Abbreviations: EPL, epipelon; EPM-M, motile epipsammon; EPM-NM, non-motile epipsammon; TYCHO, tychoplankton. Definitions and conditions of measurement of all parameters are listed in Table 2. The values for the individual species can be found in Tables S4. Values are least squares means estimates and estimated standard errors (PROC MIXED procedure).

Figure 1

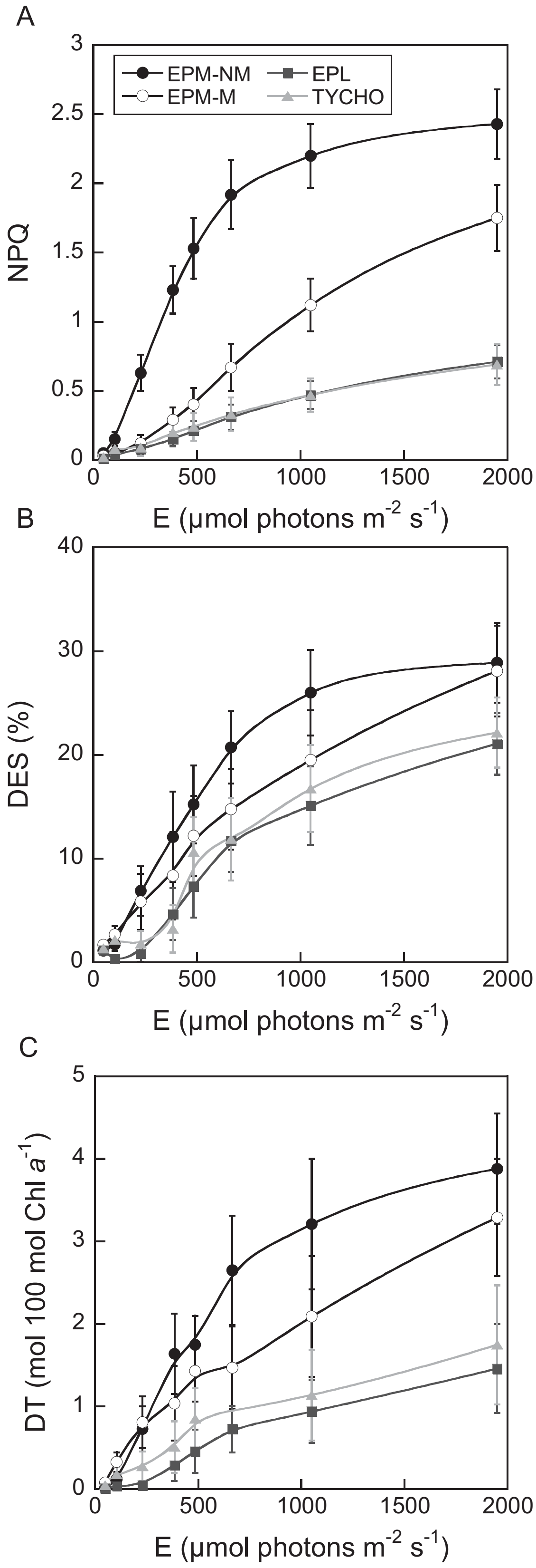
A
EPM-NM
EPM-M
EPL
TYCHO
NPQ
0
0.5
1
1.5
2
2.5
3
0
500
1000
1500
2000
E (µmol photons m^{-2} s^{-1})
B
DES (%)
0
10
20
30
40
0
500
1000
1500
2000
E (µmol photons m^{-2} s^{-1})
C
DT (mol 100 mol Chl a^{-1})
0
1
2
3
4
5
0
500
1000
1500
2000
E (µmol photons m^{-2} s^{-1})

Figure 2

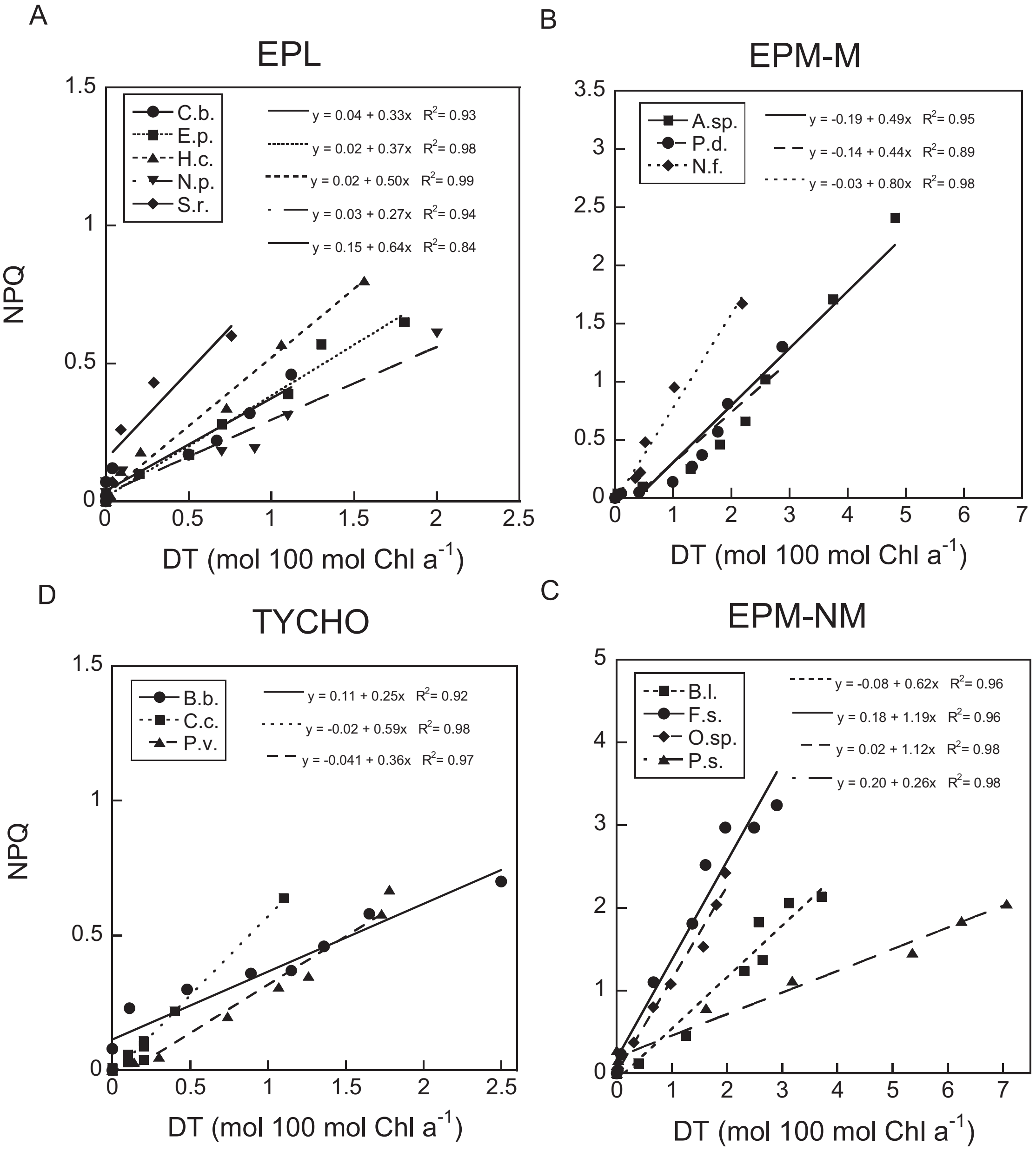
A
EPL
NPQ
DT (mol 100 mol Chl a-1)
C.b.
E.p.
H.c.
N.p.
S.r.
y = 0.04 + 0.33x R2= 0.93
y = 0.02 + 0.37x R2= 0.98
y = 0.02 + 0.50x R2= 0.99
y = 0.03 + 0.27x R2= 0.94
y = 0.15 + 0.64x R2= 0.84
0
0.5
1
1.5
2
2.5
B
EPM-M
A.sp.
P.d.
N.f.
y = -0.19 + 0.49x R2= 0.95
y = -0.14 + 0.44x R2= 0.89
y = -0.03 + 0.80x R2= 0.98
3.5
3
2.5
2
1.5
1
0.5
0
1
2
3
4
5
6
7
DT (mol 100 mol Chl a-1)
D
TYCHO
NPQ
B.b.
C.c.
P.v.
y = 0.11 + 0.25x R2= 0.92
y = -0.02 + 0.59x R2= 0.98
y = -0.041 + 0.36x R2= 0.97
DT (mol 100 mol Chl a-1)
C
EPM-NM
B.l.
F.s.
O.sp.
P.s.
y = -0.08 + 0.62x R2= 0.96
y = 0.18 + 1.19x R2= 0.96
y = 0.02 + 1.12x R2= 0.98
y = 0.20 + 0.26x R2= 0.98
5
4
3
2
1
0
DT (mol 100 mol Chl a-1)

Figure 3

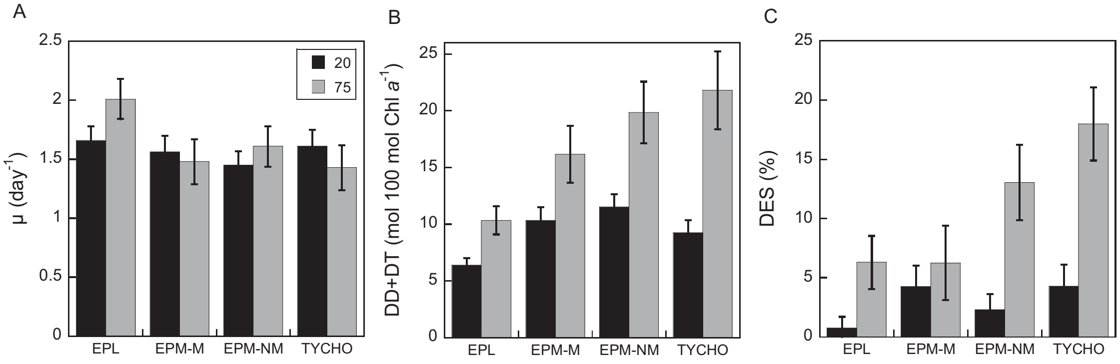
A
B
C
μ (day^{-1})
DD+DT (mol 100 mol Chl *a*$^{-1}$)
DES (%)
20
75
0
0.5
1
1.5
2
2.5
0
5
10
15
20
25
EPL
EPM-M
EPM-NM
TYCHO

Figure 4

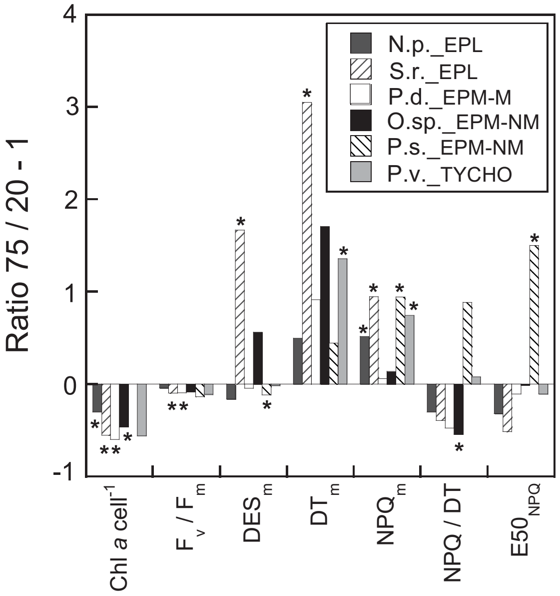
Ratio 75 / 20 - 1
4
3
2
1
0
-1
N.p._EPL
S.r._EPL
P.d._EPM-M
O.sp._EPM-NM
P.s._EPM-NM
P.v._TYCHO
*
*
*
*
*
Chl a cell^{-1}
F_v / F_m
DES_m
DT_m
NPQ_m
NPQ / DT
$E50_{NPQ}$

Figure 5

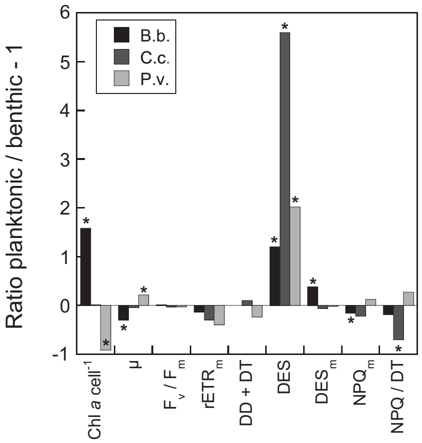
Ratio planktonic / benthic - 1
6
5
4
3
2
1
0
-1
B.b.
C.c.
P.v.
Chl *a* cell^{-1}
µ
F_v / F_m
$rETR_m$
DD + DT
DES
DES_m
NPQ_m
NPQ / DT
*

Species	Growth form		Collection n°	Sampling place	Average biovolume (µm3)
Craspedostauros britannicus C.b.	Epipelon (EPL)		NCC195-06-2	Pouliguen, Atlantic, France	1740
Entomoneis paludosa E.p.			NCC18-1	Bay of Bourgneuf, Atlantic, France	1081
Halamphora coffeaeformis H.c.			UTCC58	Victoria, British Columbia, Pacific, Canada	126
Navicula phyllepta N.p.			CCY9804	Westerschelde estuary, North sea, The Netherlands	218
Seminavis robusta S.r.			DCG 0105	Progeny of strains from Veerse Meer, The Netherlands	1790
Amphora sp. A. sp.	Epipsammon (EPM)	motile (EPM-M)	DCG 0493	Rammekenshoek, North sea, The Netherlands	39
Nitzschia cf. *frustulum* N.f.			DCG 0494	Rammekenshoek, North Sea, The Netherlands	29
Planothidium delicatulum P.d.			NCC363	Bay of Bourgneuf, Atlantic, France	242
Biremis lucens B.l.		non-motile (EPM-NM)	NCC360.2	Bay of Bourgneuf, Atlantic, France	242
Fragilaria cf. *subsalina* F.s.			DCG 0492	Rammekenshoek, North sea, The Netherlands	165
Opephora sp. O. sp.			DCG 0448	Rammekenshoek, North Sea, The Netherlands	86
Plagiogramma staurophorum P. s.			DCG 0495	Rammekenshoek, North sea, The Netherlands	n.d.
Brockmanniella brockmannii B.b.	Tychoplankton (TYCHO)		NCC161	Bay of Bourgneuf, Atlantic, France	105
Cylindrotheca closterium C.c.			Collection Univ. Aveiro	Ria de Aveiro, Atlantic, Portugal	247
Plagiogrammopsis vanheurckii P.v.			NCC186-2	Bay of Bourgneuf, Atlantic, France	737

Table 2

Parameter	Unit	Definition	Photophysiological meaning	Measurement conditions
F_0	No units	Minimum PSII Chl fluorescence yield	Used to calculate F_v/F_m (see below)	Measured with NSLCs after 15 min of dark acclimation
F_m	No units	Maximum PSII Chl fluorescence yield	Used to calculate F_v/F_m and NPQ (see below)	Measured with NSLCs during a saturating pulse after 15 min of dark acclimation
F_v/F_m	No units	Maximum photosynthetic efficiency of PSII; $F_v = F_m - F_0$	Maximum quantum ef?ciency of PSII photochemistry	See the above measurement conditions for F_0 and F_m
F_m’	No units	F_m for illuminated cells	Used to measure NPQ and rETR	Measured with NSLCs during a saturating pulse after 5 min of illumination at specific E
NPQ	No units	Non-photochemical quenching of Chl fluorescence; $NPQ = F_m / F_m' - 1$	Estimates the photoprotective dissipation of excess energy	Measured with NSLCs
rETR	µmol electrons m^{-2} s^{-1}	Relative electron transport rate of PSII; rETR = ?PSII x E where ?PSII = F_m’-F/F_m’	Effective quantum yield of photochemistry *vs*. E	Measured with RLCs; F is the steady-state of Chl fluorescence measured after 30 s illumination at a given E)
α	Relative units	rETR-E curve initial slope	Maximum light efficiency use	Derived from fitted rETR-E curves measured with RLCs (Eilers and Peeters, 1988)
$rETR_m$	µmol electrons m^{-2} s^{-1}	rETR-E curve asymptote	Maximum relative photosynthetic electron transport rate	Derived from fitted rETR-E curves measured with RLCs (Eilers and Peeters, 1988)
E_k	µmol photons. m^{-2}. s^{-1}	$E_k = rETR_m / \alpha$	Light saturation coefficient	Derived from fitted rETR-E curves measured with RLCs (Eilers and Peeters, 1988)
NPQ_m	No units	NPQ-E curve asymptote	Maximum NPQ	Measured with NSLCs
$E50_{NPQ}$	µmol photons. m^{-2}. s^{-1}	E for reaching 50% of NPQ_m	Pattern of NPQ induction *vs.* E	Derived from fitted NPQ-E curves (Serôdio and Lavaud, 2011) measured with NSLCs
n_{NPQ}	No units	NPQ-E curve sigmoidicity coefficient	Onset of NPQ induction for moderate Es (< $E50_{NPQ}$)	Derived from fitted NPQ-E curves (Serôdio and Lavaud, 2011) measured with NSLCs
DT_m	mol. 100 mol Chl *a* $^{-1}$	DT-E curve asymptote	Maximum DT concentration	Measured with NSLCs
$E50_{DT}$	µmol photons. m^{-2}. s^{-1}	E for reaching 50% of DT_{max}	Pattern of DT synthesis *vs.* E	Derived from fitted DT-E curves (Serôdio and Lavaud, 2011) measured with NSLCs
n_{DT}	No units	DT-E curve sigmoidicity coefficient	Onset of DT synthesis for moderate Es (< $E50_{NPQ}$)	Derived from fitted DT-E curves (Serôdio and Lavaud, 2011) measured with NSLCs
DES_m	%	DES-E curve asymptote; DES = [DT / (DD+DT) x 100]	Maximum de-epoxidation state	Measured with NSLCs
NPQ / DT	No units	NPQ-DT curve slope	Effective involvement of DT in NPQ for all Es (Lavaud et Lepetit, 2013)	Measured with NSLCs

Table 3

Growth Form		Pigments						Photosynthetic parameters				
	μ	Chl *a* cell^{-1}	Chl *c*	Fx	β-car	DD+DT	DES	F_v/F_m	α	rETR$_m$	E_k	PSII CET$_m$
EPL	1.66 ± 0.12	12.55 ± 12.91	18.91 ± 3.05	65.99 ± 7.90	3.91 ± 0.39	6.39 ± 0.61	0.75 ± 0.93	0.72 ± 0.01	0.68 ± 0.03	52.41 ± 5.90	78.93 ± 9.79	2.09 ± 0.23
EPM-M	1.56 ± 0.14	1.45 ± 0.78	16.05 ± 3.34	64.29 ± 10.21	2.76 ± 0.43	10.34 ± 1.17	4.25 ± 1.79	0.68 ± 0.02	0.65 ± 0.04	51.50 ± 7.36	80.41 ± 12.89	2.86 ± 0.33
EPM-NM	1.45 ± 0.12	2.13 ± 1.63	20.12 ± 3.63	70.52 ± 8.83	2.11 ± 0.43	11.52 ± 1.13	2.30 ± 1.33	0.67 ± 0.02	0.63 ± 0.04	39.20 ± 4.88	61.01 ± 8.52	2.82 ± 0.23
TYCHO	1.61 ± 0.14	1.72 ± 2.45	24.81 ± 5.17	79.36 ± 10.12	3.04 ± 0.51	9.25 ± 1.09	4.29 ± 1.83	0.73 ± 0.02	0.71 ± 0.04	58.32 ± 8.44	82.79 ± 13.40	2.03 ± 0.26

Table 4

Growth form	NPQ_m	$E50_{NPQ}$	n_{NPQ}	DES_m	DT_m	$E50_{DT}$	n_{DT}	NPQ/DT
EPL	0.69 ± 0.09	866.45 ± 200.24	1.88 ± 0.26	21.20 ± 3.38	1.34 ± 0.52	714.73 ± 128.29	2.39 ± 0.20	0.46 ± 0.10
EPM-M	1.71 ± 0.28	1061.25 ± 310.20	2.04 ± 0.34	28.68 ± 4.37	3.08 ± 1.36	809.41 ± 164.71	1.38 ± 0.20	0.52 ± 0.14
EPM-NM	2.41 ± 0.34	360.61 ± 91.42	2.27 ± 0.29	29.43 ± 3.79	3.45 ± 2.21	465.91 ± 80.04	2.30 ± 0.21	0.67 ± 0.16
TYCHO	0.66 ± 0.11	3887.42 1105.58	1.12 ± 0.34	22.73 ± 4.39	1.78 ± 0.61	1099.82 ± 341.05	1.42 ± 0.19	0.36 ± 0.10